Bull. Soc. R. Sci. Liège, 2024, **93**(2), 962–982 *Peer-reviewed conference paper*
doi:10.25518/0037-9565.11938

Observational Characteristics of Solar EUV Waves

Ramesh CHANDRA[1,*], Pooja DEVI[1], P. F. CHEN[2], Brigitte SCHMIEDER[3,4], Reetika JOSHI[5,6], Bhuwan JOSHI[7] and Arun Kumar AWASTHI[8]

[1] Department of Physics, DSB Campus, Kumaun University, Nainital 263 001, India
[2] School of Astronomy & Space Science and Key Laboratory of Modern Astronomy and Astrophysics, Nanjing University, Nanjing 210023, China
[3] LESIA, Observatoire de Paris, CNRS, 92290 Meudon Principal Cedex, France
[4] Centre for Mathematical Plasma Astrophysics, Department of Mathematics, KU Leuven, 3001 Leuven, Belgium
[5] Rosseland Centre for Solar Physics, University of Oslo, N–0315 Oslo, Norway
[6] Institute of Theoretical Astrophysics, University of Oslo, N–0315 Oslo, Norway
[7] Udaipur Solar Observatory, Physical Research Laboratory, Udaipur 313004, India
[8] Space Research Centre, Polish Academy of Sciences, Bartycka 18A, 00–716 Warsaw, Poland
[*] Corresponding author: rchandra.ntl@gmail.com

Paper presented at the 3rd BINA Workshop on "Scientific Potential of the Indo-Belgian Cooperation", held at the Graphic Era Hill University, Bhimtal (India), 22nd–24th March 2023.

Abstract

Extreme-ultraviolet (EUV) waves are one of the large-scale phenomena on the Sun. They are defined as large propagating fronts in the low corona with speeds ranging from a few tens of $\mathrm{km\,s^{-1}}$ to several $1000\,\mathrm{km\,s^{-1}}$. They are often associated with solar filament eruptions, flares, and/or coronal mass ejections (CMEs). EUV waves exhibit various features, including wave and non-wave components, stationary fronts, reflection, refraction, and mode conversion. Additionally, they can hit the nearby coronal loops and filaments/prominences during their propagation, triggering oscillations. These oscillations in loops and filaments/prominences enable us to diagnose coronal parameters such as the strength of the coronal magnetic field. In this article, we present the different observed features of the EUV waves along with existing models.

Keywords: EUV waves, coronal mass ejections, coronal oscillations

1. Introduction

Solar activities can be roughly divided into two categories, namely large and small scales. Among large-scale phenomena, Moreton waves (in the solar chromosphere) and solar extreme-ultraviolet (EUV) waves are particularly interesting and important. Moreton waves were discovered by Moreton and Ramsey (1960) in the Hα center, blue, and red wings as moving bright and dark fronts, respectively. Their reported speeds are $\sim$ 500–2000 $\mathrm{km\,s^{-1}}$. EUV waves are

defined as large propagating bright fronts clearly visible in the low corona, nearly in all directions. They were discovered by the EUV imaging telescope (EIT; Delaboudinière et al., 1995) onboard the Solar and Heliospheric Observatory (SOHO; Domingo et al., 1995) and named EIT waves. The first reported case study of EIT waves is the May 12, 1997 event, which was investigated by Thompson et al. (1998). With improved spatio-temporal resolution observations by the Solar Dynamics Observatory (SDO; Pesnell et al., 2012), there are more observations of EUV waves (e.g., Zhukov and Auchère, 2004; Chen and Wu, 2011a; Chandra et al., 2021, 2022; Devi et al., 2022b). Multi-viewpoint observations obtained with the Solar TErrestrial RElations Observatory (STEREO; Kaiser et al., 2008) twin satellite provide an opportunity to investigate the 3D structure of the phenomenon (Attrill et al., 2009; Zhukov et al., 2009a; Veronig et al., 2010; Warmuth and Mann, 2011; Long et al., 2011; Muhr et al., 2014; Long et al., 2017a; Podladchikova et al., 2019). Detailed descriptions of the EUV waves with multi-wavelength and multi-viewpoint observations have been presented in previous reviews (e.g., Warmuth, 2015 and Chen, 2016). In the past decades, EIT waves were also called EUV waves, coronal waves, solar tsunami, large-scale coronal propagating fronts, etc. According to observations, their reported speeds range from ~ 10 to more than $1000\,\mathrm{km\,s^{-1}}$. More discussion on their speed is given in Sect. 3. For consistency, we refer to them as EUV waves throughout this article. In addition to EUV wavelengths, they are also visible in radio wavelengths (Aurass et al., 2002; Pick et al., 2005; Vršnak et al., 2005; Warmuth, 2015). For radio observations, mostly data of the Nobeyama radioheliograph (NoRH; Nakajima et al., 1994) and the Nançay radioheliograph (NRH; Kerdraon and Delouis, 1997) were used. Vršnak et al. (2005) presented the radio counterparts of the EUV waves using NRH data. They found that the wave fronts are cospatial in EUV, Hα, and X-rays. The development of the EUV wave observed at different NRH frequencies was also presented by Pick et al. (2005). The radio signatures of EUV waves were also observed in the microwave range with the NoRH dataset at 17 GHz by Aurass et al. (2002) and Warmuth et al. (2004).

Regarding the association of EUV waves with solar flares or coronal mass ejections (CMEs), it is now believed that EUV waves are closely associated with CMEs. The association between EUV waves and CMEs was initially investigated by Biesecker et al. (2002), who found a strong correlation between them, whereas the association with solar flares is weaker. Using data from the EIT and the Large Angle and Spectroscopic Coronagraph (LASCO; Brueckner et al., 1995), Kay et al. (2003) examined 69 ejective and non-ejective flares and found that all EUV wave-associated flares are accompanied by CMEs. Chen (2006) selected a set of 14 non-CME-associated flares, focusing on energetic flares as they are excepted to generate stronger pressure pulses. It was found that none of the selected flares are associated with EUV waves. Chen (2009) examined an EUV wave and its association with CME using the data of EIT and the high-cadence Mark-III K–Coronagraph (MK3) at the Mauna Loa Solar Observatory (MLSO; Fisher et al., 1981). He found that EUV wave fronts and CME leading fronts are well-coaligned. With the SDO observational data sets, other authors have also investigated the association of CMEs with EUV waves, finding that the association rate varies from 65 to 79 % (Nitta et al., 2013, 2014; Muhr et al., 2014). The minimum association rate of 65 % is from Nitta et al. (2013), who focused solely on solar disk EUV waves.

In the following sections, we present an overview of the existing EUV wave models and their different observational evidence. The paper is organized as follows: Section 2 presents a brief summary of existing models. Different observational features are described in Sect. 3. The utilization of EUV waves for coronal seismology is given in Sect. 4. Finally, a brief summary is presented in Sect. 5.

2. Existing Models

Since the discovery of EUV waves, several models have been proposed by different investigators. The main models include wave, non-wave, and hybrid models, which are briefly described below.

2.1. Wave model

Initially, upon their discovery, EUV waves – then known as EIT waves – were assumed to be fast-mode MHD waves or shock waves (Thompson et al., 1999; Wang, 2000; Wu et al., 2001; Warmuth et al., 2001; Ofman and Thompson, 2002). It was believed that they are the coronal counterparts of Moreton waves (e.g., Asai et al., 2012). Uchida (1968) developed a numerical MHD model to explain Moreton waves, suggesting that the shock wave is generated by the high-pressure pulse in the flaring loops. It was, however, later pointed out that the shock wave may not be due to the pressure pulse, and should be piston-driven by an erupting filament or CME (Chen et al., 2002). In addition to the fast-mode wave model, alternative models such as the slow-mode soliton model (Wills-Davey et al., 2007) and magneto-acoustic surface gravity waves (Ballai et al., 2011) were also proposed. Observational features such as reflection, transmission, refraction, and mode conversion tend to support the existence of a wave component in EUV waves, as discussed in Sect. 3 of this article.

2.2. Non-wave model

After the discovery of EUV waves, numerous studies have been conducted using various instruments worldwide. In particular, research on EUV waves became more elaborate following the launch of the Atmospheric Imaging Assembly (AIA; Lemen et al., 2012) onboard SDO. Many peculiar features of this phenomenon have been reported. Analyzing the temporal evolution of EUV waves, studies have found that the estimated speeds, obtained through manual tracking as well as time-distance techniques, vary from tens to more than 1000 $\mathrm{km\,s^{-1}}$ (Thompson et al., 2000; Zhukov and Auchère, 2004; Chen, 2009; Nitta et al., 2013; Chandra et al., 2018, 2021, and references therein). For the first time, Delannée and Aulanier (1999) reported stationary fronts associated with the EUV waves using data from the EIT instrument. They also noticed that this stationary brightening is co-spatial with a magnetic quasi-separatrix layer (QSL). The very low speed of EUV waves, together with the reported stationary fronts, raises doubts about the wave nature of EUV waves. To explain the stationary fronts of EUV waves, Delannée and Aulanier (1999) proposed the non-wave model (also known as the magnetic reconfiguration model). According to this model, the consequence of the reconfiguration of the

magnetic field is due to the eruption of CMEs. Delannée and Aulanier (1999) conjectured that an EUV wave is the disk projection of the expanding CME. Based on further 3D MHD simulations, they proposed a current shell model to explain the EUV waves. In their simulations, they found that due to an erupting flux rope, a current shell forms around it, and because of the Joule heating of the current shell, the EUV wave is observed. A successive reconnection model was also proposed to explain EUV waves (Attrill et al., 2007; van Driel-Gesztelyi et al., 2008; Cohen et al., 2009, 2010). According to this model, the EUV wave results from the reconnection between the expanding CME and quiet magnetic loops (see Fig. 4 of Attrill et al., 2007).

2.3. Hybrid model

On the one hand, solar flares/CMEs can indeed drive fast-mode waves; on the other hand, multi-wavelength and multi-vantage observations have revealed many characteristics in EUV waves that cannot be accounted for by any wave model (Delannée and Aulanier, 1999; Warmuth et al., 2004; Balasubramaniam et al., 2005; Attrill et al., 2007; Delannée et al., 2007). Bearing this in mind, Chen et al. (2002, 2005) performed MHD numerical simulations of flux rope eruptions (see their Figs. 7 and 8). They found that after a flux rope erupts, two wavelike phenomena with different speeds are observed in the solar corona. The faster wave is a piston-driven shock wave propagating ahead of the erupting flux rope. The leg of this wave travels outward in the horizontal direction and was explained as the coronal Moreton wave, i.e., the wave component of the EUV waves. The slower wavelike features also propagate outward but behind the faster component of the EUV waves. They claimed that the slower component corresponds to the EIT wave observed for the first time by the EIT onboard the SOHO satellite. To explain the formation of the slower component of the EUV waves, they proposed a hybrid model, wherein an erupting flux rope would generate two types of EUV waves, or there are two components of EUV waves. The faster one is a fast-mode MHD wave or shock wave and the slower component, i.e., the non-wave component, is generated due to the successive stretching of magnetic field lines straddling over the erupting flux rope. Since this model explains both the wave and the non-wave components of the EUV waves, it is known as a hybrid model. Very recently, Guo et al. (2023) performed a 3D data-driven MHD simulation of the October 28, 2021 EUV wave event. They confirmed the coexistence of two components of EUV waves predicted by the magnetic stretching model. They also verified the cospatiality between the CME piston-driven shock and the fast EUV wave component, together with the cospatiality between the CME leading front and the non-wave component of the EUV waves.

3. Observational Features

The observational features of EUV waves are explained as follows.

3.1. Two Components

EUV waves were discovered by the EIT instrument onboard the SOHO satellite, and researchers calculated their speeds. The first reported EUV wave event on May 12, 1997 was

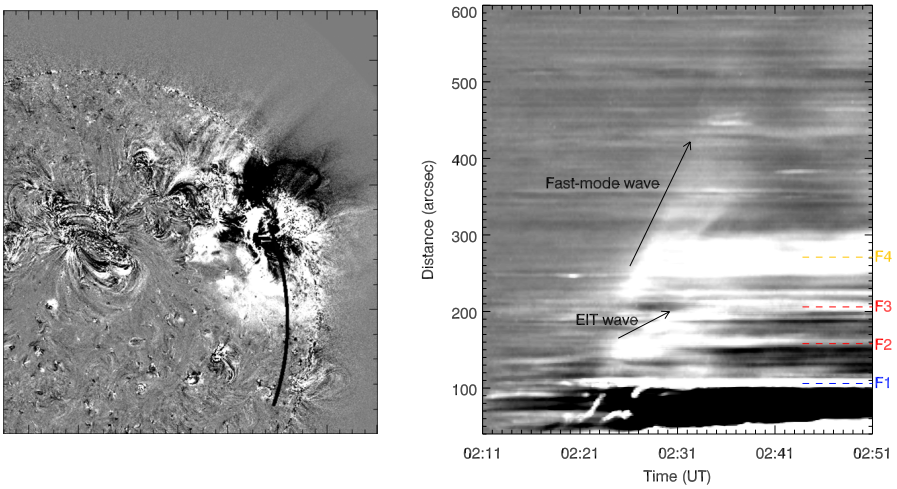

Figure 1: (*left*) AIA 193 Å difference image on May 11, 2011 at 02:11 UT. (*right*) Time-distance plot along the curved slice and location of the fast, non-wave component along with stationary fronts F1–F4. (Adapted from Chandra et al., 2016).

studied by Thompson et al. (1998) with lower temporal resolution. By tracking the wave leading edges in different directions, the measured speed of the EUV wave was 245 km s^{-1}. Further statistical studies on EUV waves using SOHO/EIT and STEREO/EUVI found average speeds of 200–500 km s^{-1} (Klassen et al., 2000; Thompson and Myers, 2009; Muhr et al., 2014). On the other hand, some authors found the speeds of some EUV waves to be less than the sound speed in the corona (Tripathi and Raouafi, 2007; Thompson and Myers, 2009), and in some cases, it is only $\sim$ 10 km s^{-1} (Zhukov et al., 2009b). These observations actually imply the existence of two types of EUV waves (Chen, 2016). For the first time, the observations of two components of an EUV wave were reported by Harra and Sterling (2003) using the better time resolution data (1 to 2 min) of the Transition Region and Coronal Explorer (TRACE; Handy et al., 1999) satellite. They reported that the faster and slower component front speeds are $\sim$ 500 km s^{-1} and $\sim$ 200 km s^{-1}, respectively. They also reported that the faster front is fainter than the slower front.

Due to the low temporal resolutions of the earlier observations, the two components of EUV waves, as predicted by the hybrid model, could not be clearly distinguished. It is possible that, due to the high speed of the fast-mode wave component, it had already traveled out of the field of view (FOV) of observing instruments. Before being observed with the high spatio-temporal resolution SDO data, several events were analyzed, and the speeds of the EUV waves were calculated using the time-distance technique. Many studies provided evidence of the two components of EUV waves (Chen and Wu, 2011b; Asai et al., 2012; White et al., 2013; Guo et al., 2015). However, some EUV wave events do not show both components together (Nitta et al., 2013; Hou et al., 2022; Wang et al., 2022; Zheng et al., 2022). An example of the existence of two components of EUV waves is displayed in Fig. 1. The faster component of the EUV waves is a real MHD wave while the slower component is the non-wave component (or previously reported EIT wave). According to the hybrid model, the faster front is interpreted as a fast-mode

MHD wave or shock wave and the inner slower component corresponds to plasma compression due to successive stretching of magnetic field lines which are pushed by an erupting flux rope. Using the two view-point observations of AIA and STEREO–B instruments, Chandra et al. (2021) confirmed the existence of the fast-mode and non-wave components of EUV waves. They found that the location of non-wave component spatially coincides with the non-wave component observed by STEREO–B. Regarding the speeds of wave and non-wave components of the EUV waves, Chen (2016) presented excellent discussions. According to him, the wave whose speed is greater than $500\,\mathrm{km\,s^{-1}}$ is a fast-mode wave and that less than $300\,\mathrm{km\,s^{-1}}$ is non-wave in nature. If the speed is between these two limits, i.e., 300 to $500\,\mathrm{km\,s^{-1}}$, it is difficult to determine the nature of the wave. In this case, the nature of wave depends upon other kinematics properties such as whether it stops near the QSLs, and its refraction/reflection when encountering magnetic features.

3.2. Stationary Fronts

Delannée and Aulanier (1999) were the first to report the existence of brightening persisting for several hours in the same location. This phenomenon, now well-known as stationary brightening, was further investigated by Delannée (2000), who extended their study and reported more cases of stationary brightening. Utilizing the high temporal and spatial resolution data of AIA onboard SDO, Chen and Wu (2011b) analyzed the EUV wave event of July 27, 2010, and presented the temporal evolution of the wave with a time-distance diagram along the selected artificial slices. They also observed the stationary front associated with the non-wave component in the time-distance diagram located $250''$ from the flare site. They investigated the magnetic topology of the stationary front and identified a magnetic separatrix at that location. Delannée et al. (2008) explained the stationary fronts by the current shell model. On the other hand, such stationary brightenings can also be explained by the magnetic field-line stretching model of Chen et al. (2002, 2005). Chandra et al. (2016) analyzed the event of May 11, 2011, and reported several stationary fronts. They also compared their locations with the PFSS extrapolated magnetic field and found that their locations are very close to magnetic separatrices, as expected in the magnetic field-line stretching model. Some of the stationary fronts are shown in Fig. 1.

3.3. Mode conversion

As mentioned earlier, stationary fronts were initially observed as the final position of the non-wave component of EUV waves. Furthermore, Chandra et al. (2016) were the first to analyze an EUV wave event and they reported that, in addition to the non-wave component, a fast-mode component of EUV waves also generated a stationary front close to a QSL. Based on their observations, they tentatively proposed a wave-trapping model. According to their interpretation, as a fast-mode wave propagates across a magnetic QSL, part of the fast-mode wave is trapped inside the cavity while the rest moves ahead. It is well-known that when a fast-mode wave penetrates into a region of weak magnetic field (where the Alfvén speed is comparable to the sound speed), a portion of the fast-mode wave converts into a slow-mode

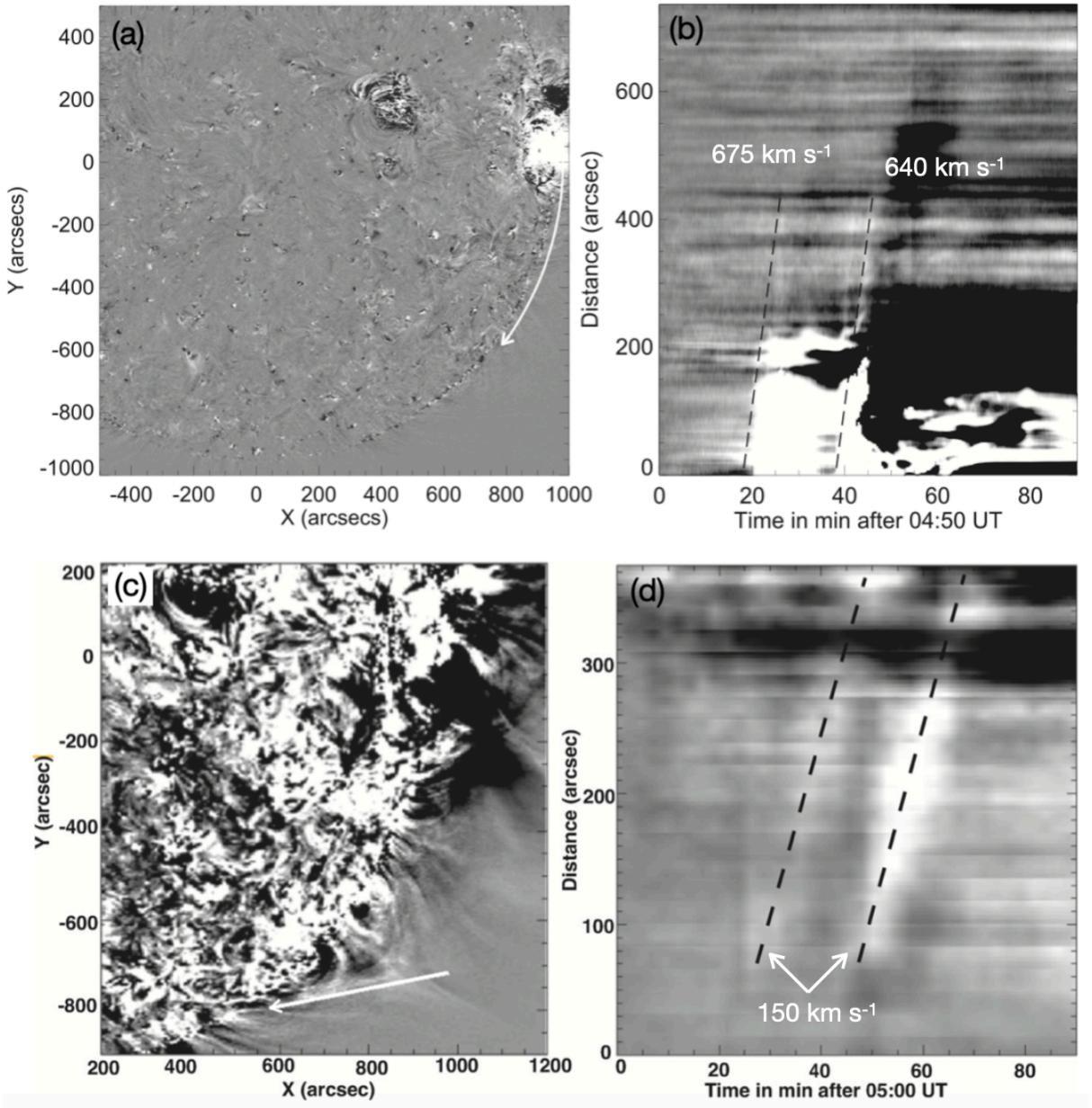

Figure 2: EUV wave mode conversion through helmet streamer on July 23, 2016. The figure displays the locations of slits and corresponding time-distance plots. Panels (a) and (c) show AIA 193 Å images captured at 05:12 and 05:59 UT, respectively. (Adapted from Chandra et al., 2018).

wave (Cally, 2005). Such a mode conversion can also happen in solar coronal conditions. Keeping this fact in mind and motivated by the observational features reported by Chandra et al. (2016), Chen et al. (2016) conducted numerical simulations to interact the interaction between a fast-mode wave and a magnetic QSL. Their simulations revealed that when the fast-mode shock wave enters a region with a weak magnetic field around a QSL, it undergoes partial conversion into a slow-mode wave. Subsequently the slow-mode wave travels along the magnetic field lines with the local sound speed. Eventually, the slow-mode wave halts at a location in front of the magnetic separatrix. Subsequent observations of stationary fronts at magnetic QSLs were made by Fulara et al. (2019). They found that the fast-mode component of the EUV waves encounters two QSLs, and stationary fronts are observed at both QSL locations (refer to their Fig. 11).

Later, more examples of mode conversion have been reported in EUV wave events (Zong and Dai, 2017; Chandra et al., 2018; Zheng et al., 2018). In the study by Zong and Dai (2017), the fast-mode wave interacts with the coronal cavity, resulting in its conversion into a slow-mode wave. According to Chandra et al. (2018), two fast-component EUV waves originating from two filament eruptions were both converted into slow-mode waves. Zheng et al. (2018) also observed mode conversion when fast-mode EUV waves interacted with coronal streamers, referring to it as 'secondary wave'. It is noteworthy that the tips of the helmet streamers and coronal cavity map to magnetic QSLs, and their low Alfvén speeds facilitate mode conversion. One example of EUV wave mode conversions at the helmet streamers is presented in Fig. 2.

3.4. Reflection and refraction

Reflection and refraction serve as strong evidence for the presence of a fast-mode wave component in EUV waves. Reflection occurs around coronal holes (CHs), active regions (ARs), and helmet streamers (Long et al., 2008; Veronig et al., 2008; Gopalswamy et al., 2009). This phenomenon was discovered using STEREO data nearly a decade after the initial discovery of EUV waves. The long delay in reporting the reflection phenomena (which is very common for waves) may be attributed to the lower cadence of the EIT telescope. It was immediately reported after the availability of STEREO data, which provided improved temporal resolution observations. This confirms the conjecture that the fast-mode EUV wave component was missed by the low cadence observations, as seen in the case of EIT datasets. Gopalswamy et al. (2009) demonstrated the reflection of an EUV wave from a CH using the time-distance diagram. Following the launch of the SDO satellite, a large number of EUV wave reflection cases were reported at various magnetic structures on the solar surface, such as CHs, ARs, and bright points (Li et al., 2012; Olmedo et al., 2012; Yang et al., 2013; Shen et al., 2013). Total reflection was observed in the case of the December 22, 2015 event by Zhou et al. (2022) from the CH boundary. Their observational results indicated that the reflection was total because the measured incidence and critical angles satisfied the theory of total reflection, where the incident angle is greater than the critical angle. Yang et al. (2013) investigated an example of wave reflection through a CH and an AR in a single event that occurred on August 04, 2011, as presented in Fig. 3. However, it should be noted that not all CHs reflect EUV waves (Chandra et al., 2022). Thompson et al.

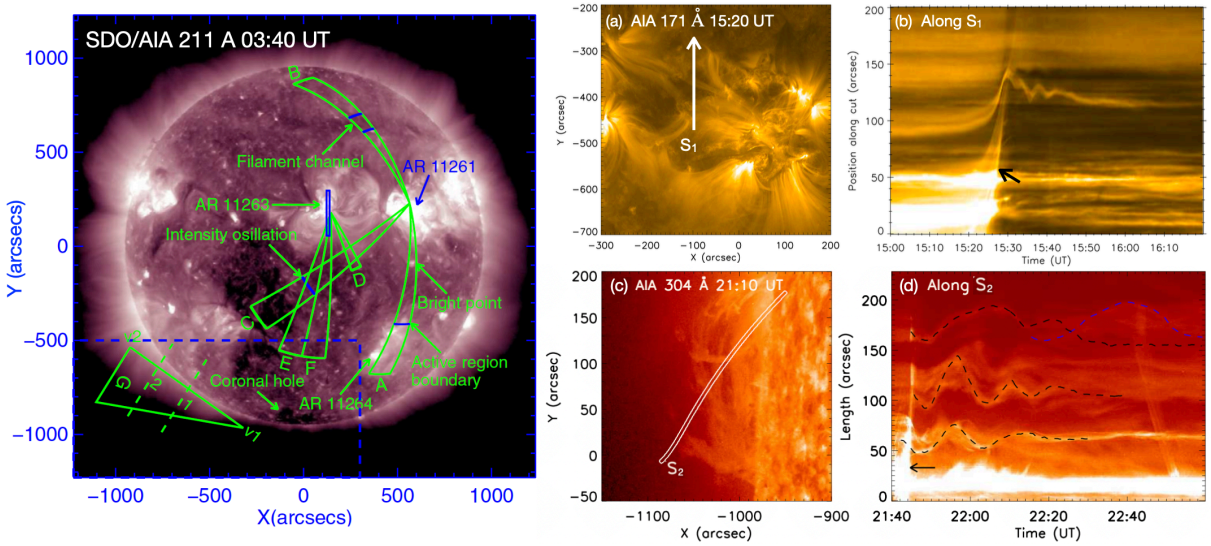

Figure 3: (*left*) EUV wave reflection though CH and AR on August 04, 2011 represents by sectors C–F (adapted from Yang et al., 2013). (*right*) Loop oscillation on October 28, 2021 with slit S_1 and corresponding time-distance plot are shown in (a) and (b). Prominence oscillations created by the EUV wave on February 11, 2011 with slit S_2 and the time-distance plot are shown in (c) and (d). Black arrows show the EUV waves. (Adapted from Devi et al., 2022a,b).

(2000) reported the refraction of the EUV wave from an AR for the first time. Subsequently, the refraction of EUV waves was observed by many other authors (Wills-Davey and Thompson, 1999; Ofman and Thompson, 2002; Shen and Liu, 2012; Yang et al., 2013; Liu et al., 2018). Using 2.5D MHD simulations of the interactions of a fast-mode MHD wave with CHs, Piantschitsch and coworkers revealed phenomena of reflection, refraction, and transmission of the wave during its interaction with CHs (Piantschitsch et al., 2017, 2018a,b). Additionally, in 3D MHD simulations, Ofman and Thompson (2002) also reported the reflection, refraction, and dissipation of the wave with small transmission after the interaction of MHD wave with an AR.

4. Coronal Seismology

As an EUV wave begins propagating on or above the solar disk, its faster component reflects the local fast-mode MHD wave speed. This characteristic makes it possible to derive the coronal magnetic field. Additionally, it can interact with magnetic structures such as coronal loops and solar filaments, potentially disturbing them. Consequently, these structures can either oscillate or erupt. If they oscillate, they can offer valuable information that can be utilized to determine the various physical parameters of the corona, including the magnetic-field strength (B), plasma density, transport coefficients, and heating functions, through a technique known as coronal seismology (Uchida, 1970; Roberts et al., 1984; Nakariakov and Ofman, 2001; Nakariakov and Verwichte, 2005). Mann et al. (1999) were the first to apply this technique to measure B; considering the coronal transient wave to be a fast magnetosonic wave. They derived the

Alfvén speed (v_A) by using the relation $V_{wave} = \sqrt{v_A^2 + c_s^2}$, where V_{wave} is the speed of the EUV wave and c_s the coronal sound speed. v_A is then utilized to calculate B by using the formula, $B = v_A\sqrt{4\pi\mu m_p N}$ (in CGS units). Here, $N = N_e/0.52$ (Newkirk, 1961) denotes the particle number density, N_e is the electron density, $\mu = 0.6$, and m_p is the mass of the proton. By using the period and length of oscillating loops, the ratio of the densities inside (n_{in}) and outside (n_{ex}) the loops can be estimated with the relation $\frac{n_{in}}{n_{ex}} = \frac{1}{2}\left(v\frac{P}{L}\right) - 1$ (Aschwanden and Schrijver, 2011), where v is the global fast magneto-acoustic wave speed, and P and L denote the period and length of the oscillating loops, respectively.

Using the wave kinematics, several authors have derived the lower coronal magnetic field (Warmuth et al., 2005; Ballai, 2007; Devi et al., 2022a). Their measured values typically range from 0.5 to 8 G. Devi et al. (2022a) analyzed the interaction of EUV waves with neighboring EUV loops and their resulting oscillations, finding that the coronal magnetic field ranges from 1 to 8 G. In another study, Devi et al. (2022b) presented the oscillations of a prominence caused by an EUV wave and calculated the magnetic field strength within the prominence. The calculated magnetic field values range from 14 to 20 G, consistent with previous studies (Mackay et al., 2010; Luna et al., 2017). Figure 3 illustrates an example of oscillating EUV loops and filaments along with their time-distance diagrams. It would be interesting to compare the magnetic field strength computed using seismology with radio observational techniques as well as modeling.

5. Summary

In this article, we have provided a review of the recent observational results of the EUV wave events and modelings. The main points of this review are summarized as follows.

- An EUV wave event is often composed of two components: a fast-mode wave and a non-wave component. Both of these components can be effectively explained by the hybrid model.
- The fast-mode wave component of EUV waves was substantiated by its reflection, refraction, and mode conversion characteristics. The reflection, refraction, and mode conversion were observed at the boundaries of coronal holes (CHs), active regions (ARs), and helmet streamers, which frequently coincide with magnetic quasi-separatrix layers (QSLs).
- The observations of stationary brightening, which are associated with the slower component of EUV waves, provide evidence for the existence of non-wave components within EUV waves.
- Propagating EUV waves have the potential to interact with magnetic structures within the solar corona, potentially inducing oscillations or eruptions of coronal structures. Consequently, this interaction enables the tracing of plasma and magnetic fields within various coronal structures.

It should be noted that the separation between the wave and non-wave components is very useful and interesting, as it can help clarify the association among EUV waves, type II radio bursts, and solar energetic particle (SEP) events. Type II radio bursts result from the shock wave ahead of a CME. Therefore, if EUV waves are the fast-mode shock waves driven by eruptions, they should be strongly correlated with type II radio bursts. However, many studies have found a weak correlation between the speeds of these two phenomena (Klassen et al., 2000; Long et al., 2017b). The reason for the negative results is that those authors treated the EIT waves – which constitute the non-wave component of EUV waves – as fast-mode shock waves. Similarly, some authors tried to associate EIT waves with SEPs (Bothmer et al., 1997; Torsti et al., 1999; Miteva et al., 2014). In our opinion, such attempts may only yield meaningful results if the wave and non-wave components of EUV waves are separated. Only the faster component EUV wave can provide correct information associated with type II radio bursts and SEPs.

Certainly, further efforts are required to explore the relationship between CMEs and EUV waves. For this purpose, the CME and EUV observations should have overlapping fields of view to the greatest extent possible. Ground-based coronagraphs like MLSO MK3, MK4, and the currently working MLSO KCor can be highly valuable for this purpose. However, it's important to note that ground-based telescopes are limited by their duty cycle in observations. Therefore, we believe that observations of CMEs in the inner corona from space platforms are necessary. The recently launched Indian spacecraft ADITYA–L1, equipped with its Visible Emission Line Coronagraph (VELC) instrument, holds significant potential to provide essential observations for a more detailed understanding of these phenomena.

Acknowledgments

The authors thank the open data policy of the SDO and STEREO, and SOHO teams. P.F.C. is financially supported by the National Key Research and Development Program of China (2020YFC22-01200) and NSFC (12127901). P.D. is supported by CSIR, New Delhi. R.J. acknowledges the support by the Research Council of Norway through its Centres of Excellence scheme, project number 262622. R.C. acknowledges the support from SERB/DST, project no. EEQ/2023/000214, Govt. of India, New Delhi. We acknowledge the BINA conference organized at Nainital, India. We thank the referee for the comments and suggestions.

Further Information

Authors' ORCID identifiers

0000-0002-3518-5856 (Ramesh CHANDRA)
0000-0003-0713-0329 (Pooja DEVI)
0000-0002-7289-642X (P. F. CHEN)
0000-0003-3364-9183 (Brigitte SCHMIEDER)
0000-0003-0020-5754 (Reetika JOSHI)

0000-0001-5042-2170 (Bhuwan JOSHI)
0000-0003-1948-1548 (Arun Kumar AWASTHI)

Author contributions

R.C., P.D., B.S., B.J., R.J., and A.K.A. contributed to the data analysis. R.C. wrote the main draft of the paper. P.F.C. wrote substantial parts of the manuscript and contributed to the interpretation. All the authors did a careful proofreading of the text and references.

Conflicts of interest

The authors declare no conflict of interest.

References

Asai, A., Ishii, T. T., Isobe, H., Kitai, R., Ichimoto, K., UeNo, S., Nagata, S., Morita, S., Nishida, K., Shiota, D., Oi, A., Akioka, M. and Shibata, K. (2012) First simultaneous observation of an Hα Moreton wave, EUV wave, and filament/prominence oscillations. ApJ, 745, L18. https://doi.org/10.1088/2041-8205/745/2/L18.

Aschwanden, M. J. and Schrijver, C. J. (2011) Coronal loop oscillations observed with Atmospheric Imaging Assembly–kink mode with cross-sectional and density oscillations. ApJ, 736(2), 102. https://doi.org/10.1088/0004-637X/736/2/102.

Attrill, G. D. R., Engell, A. J., Wills-Davey, M. J., Grigis, P. and Testa, P. (2009) Hinode/XRT and STEREO observations of a diffuse coronal "wave"–coronal mass ejection-dimming event. ApJ, 704, 1296–1308. https://doi.org/10.1088/0004-637X/704/2/1296.

Attrill, G. D. R., Harra, L. K., van Driel-Gesztelyi, L. and Démoulin, P. (2007) Coronal "wave": Magnetic footprint of a coronal mass ejection? ApJ, 656, L101–L104. https://doi.org/10.1086/512854.

Aurass, H., Shibasaki, K., Reiner, M. and Karlický, M. (2002) Microwave detection of shock and associated electron beam formation. ApJ, 567(1), 610–621. https://doi.org/10.1086/338417.

Balasubramaniam, K. S., Pevtsov, A. A., Neidig, D. F., Cliver, E. W., Thompson, B. J., Young, C. A., Martin, S. F. and Kiplinger, A. (2005) Sequential chromospheric brightenings beneath a transequatorial halo coronal mass ejection. ApJ, 630(2), 1160–1167. https://doi.org/10.1086/432030.

Ballai, I. (2007) Global coronal seismology. SoPh, 246, 177–185. https://doi.org/10.1007/s11207-007-0415-3.

Ballai, I., Forgács-Dajka, E. and Douglas, M. (2011) Magnetoacoustic surface gravity waves at a spherical interface. A&A, 527, A12. https://doi.org/10.1051/0004-6361/201016075.

Biesecker, D. A., Myers, D. C., Thompson, B. J., Hammer, D. M. and Vourlidas, A. (2002) Solar phenomena associated with "EIT waves". ApJ, 569(2), 1009–1015. https://doi.org/10.1086/339402.

Bothmer, V., Posner, A., Kunow, H., Müller-Mellin, R., Herber, B., Pick, M., Thompson, B. J., Delaboudinière, J. P., Brueckner, G. E., Howard, R. A., Michels, D. J., Cyr, C. S., Szabo, A., Hudson, H. S., Mann, G., Classen, H. T. and McKenna-Lawlor, S. (1997) Solar energetic particle events and coronal mass ejections: New insights from SOHO. In Correlated Phenomena at the Sun, in the Heliosphere and in Geospace, edited by Wilson, A., vol. 415 of *ESASP*, pp. 207–216. https://ui.adsabs.harvard.edu/abs/1997ESASP.415..207B.

Brueckner, G. E., Howard, R. A., Koomen, M. J., Korendyke, C. M., Michels, D. J., Moses, J. D., Socker, D. G., Dere, K. P., Lamy, P. L., Llebaria, A., Bout, M. V., Schwenn, R., Simnett, G. M., Bedford, D. K. and Eyles, C. J. (1995) The Large Angle Spectroscopic Coronagraph (LASCO). SoPh, 162, 357–402. https://doi.org/10.1007/BF00733434.

Cally, P. S. (2005) Local magnetohelioseismology of active regions. MNRAS, 358(2), 353–362. https://doi.org/10.1111/j.1365-2966.2005.08742.x.

Chandra, R., Chen, P. F., Devi, P., Joshi, R. and Ni, Y. W. (2022) Dynamics and kinematics of the EUV wave event on 6 May 2019. Galax, 10(2), 58. https://doi.org/10.3390/galaxies10020058.

Chandra, R., Chen, P. F., Devi, P., Joshi, R., Schmieder, B., Moon, Y.-J. and Uddin, W. (2021) Fine structures of an EUV wave event from multi-viewpoint observations. ApJ, 919(1), 9. https://doi.org/10.3847/1538-4357/ac1077.

Chandra, R., Chen, P. F., Fulara, A., Srivastava, A. K. and Uddin, W. (2016) Peculiar stationary EUV wave fronts in the eruption on 2011 May 11. ApJ, 822(2), 106. https://doi.org/10.3847/0004-637X/822/2/106.

Chandra, R., Chen, P. F., Joshi, R., Joshi, B. and Schmieder, B. (2018) Observations of two successive EUV waves and their mode conversion. ApJ, 863(1), 101. https://doi.org/10.3847/1538-4357/aad097.

Chen, P. F. (2006) The relation between EIT waves and solar flares. ApJ, 641(2), L153–L156. https://doi.org/10.1086/503868.

Chen, P. F. (2009) The relation between EIT waves and coronal mass ejections. ApJ, 698, L112–L115. https://doi.org/10.1088/0004-637X/698/2/L112.

Chen, P. F. (2016) Global coronal waves. GMS, 216, 381–394. https://doi.org/10.1002/9781119055006.ch22.

Chen, P. F., Fang, C., Chandra, R. and Srivastava, A. K. (2016) Can a fast-mode EUV wave generate a stationary front? SoPh, 291, 3195–3206. https://doi.org/10.1007/s11207-016-0920-3.

Chen, P. F., Fang, C. and Shibata, K. (2005) A full view of EIT waves. ApJ, 622, 1202–1210. https://doi.org/10.1086/428084.

Chen, P. F., Wu, S. T., Shibata, K. and Fang, C. (2002) Evidence of EIT and Moreton waves in numerical simulations. ApJ, 572, L99–L102. https://doi.org/10.1086/341486.

Chen, P. F. and Wu, Y. (2011a) First evidence of coexisting EIT wave and coronal Moreton wave from *SDO*/AIA observations. ApJ, 732, L20. https://doi.org/10.1088/2041-8205/732/2/L20.

Chen, P. F. and Wu, Y. (2011b) First evidence of coexisting EIT wave and coronal Moreton wave from SDO/AIA observations. ApJ, 732, L20. https://doi.org/10.1088/2041-8205/732/2/L20.

Cohen, O., Attrill, G. D. R., Manchester, I., Ward B. and Wills-Davey, M. J. (2009) Numerical simulation of an EUV coronal wave based on the 2009 February 13 CME event observed by STEREO. ApJ, 705(1), 587–602. https://doi.org/10.1088/0004-637X/705/1/587.

Cohen, O., Attrill, G. D. R., Schwadron, N. A., Crooker, N. U., Owens, M. J., Downs, C. and Gombosi, T. I. (2010) Numerical simulation of the 12 May 1997 CME event: The role of magnetic reconnection. JGR, 115(A10), A10104. https://doi.org/10.1029/2010JA015464.

Delaboudinière, J. P., Artzner, G. E., Brunaud, J., Gabriel, A. H., Hochedez, J. F., Millier, F., Song, X. Y., Au, B., Dere, K. P., Howard, R. A., Kreplin, R., Michels, D. J., Moses, J. D., Defise, J. M., Jamar, C., Rochus, P., Chauvineau, J. P., Marioge, J. P., Catura, R. C., Lemen, J. R., Shing, L., Stern, R. A., Gurman, J. B., Neupert, W. M., Maucherat, A., Clette, F., Cugnon, P. and Van Dessel, E. L. (1995) EIT: Extreme-ultraviolet Imaging Telescope for the SOHO mission. SoPh, 162(1-2), 291–312. https://doi.org/10.1007/BF00733432.

Delannée, C. (2000) Another view of the EIT wave phenomenon. ApJ, 545(1), 512–523. https://doi.org/10.1086/317777.

Delannée, C. and Aulanier, G. (1999) CME associated with transequatorial loops and a bald patch flare. SoPh, 190, 107–129. https://doi.org/10.1023/A:1005249416605.

Delannée, C., Hochedez, J.-F. and Aulanier, G. (2007) Stationary parts of an EIT and Moreton wave: a topological model. A&A, 465, 603–612. https://doi.org/10.1051/0004-6361:20065845.

Delannée, C., Török, T., Aulanier, G. and Hochedez, J.-F. (2008) A new model for propagating parts of EIT waves: A current shell in a CME. SoPh, 247, 123–150. https://doi.org/10.1007/s11207-007-9085-4.

Devi, P., Chandra, R., Awasthi, A. K., Schmieder, B. and Joshi, R. (2022a) Extreme-ultraviolet wave and accompanying loop oscillations. SoPh, 297(12), 153. https://doi.org/10.1007/s11207-022-02082-6.

Devi, P., Chandra, R., Joshi, R., Chen, P. F., Schmieder, B., Uddin, W. and Moon, Y.-J. (2022b) Prominence oscillations activated by an EUV wave. AdSpR, 70(6), 1592–1600. https://doi.org/10.1016/j.asr.2022.02.053.

Domingo, V., Fleck, B. and Poland, A. I. (1995) The SOHO mission: an overview. SoPh, 162, 1–37. https://doi.org/10.1007/BF00733425.

Fisher, R. R., Lee, R. H., MacQueen, R. M. and Poland, A. I. (1981) New Mauna Loa coronagraph systems. ApOpt, 20(6), 1094–1101. https://doi.org/10.1364/AO.20.001094.

Fulara, A., Chandra, R., Chen, P. F., Zhelyazkov, I., Srivastava, A. K. and Uddin, W. (2019) Kinematics and energetics of the EUV waves on 11 April 2013. SoPh, 294(5), 56. https://doi.org/10.1007/s11207-019-1445-3.

Gopalswamy, N., Yashiro, S., Temmer, M., Davila, J., Thompson, W. T., Jones, S., McAteer, R. T. J., Wuelser, J. P., Freeland, S. and Howard, R. A. (2009) EUV wave reflection from a coronal hole. ApJ, 691(2), L123–L127. https://doi.org/10.1088/0004-637X/691/2/L123.

Guo, J. H., Ni, Y. W., Zhong, Z., Guo, Y., Xia, C., Li, H. T., Poedts, S., Schmieder, B. and Chen, P. F. (2023) Thermodynamic and magnetic topology evolution of the X1.0 flare on 2021 October 28 simulated by a data-driven radiative magnetohydrodynamic model. ApJS, 266(1), 3. https://doi.org/10.3847/1538-4365/acc797.

Guo, Y., Ding, M. D. and Chen, P. F. (2015) Slow patchy extreme-ultraviolet propagating fronts associated with fast coronal magneto-acoustic waves in solar eruptions. ApJS, 219(2), 36. https://doi.org/10.1088/0067-0049/219/2/36.

Handy, B. N., Acton, L. W., Kankelborg, C. C., Wolfson, C. J., Akin, D. J., Bruner, M. E., Caravalho, R., Catura, R. C., Chevalier, R., Duncan, D. W., Edwards, C. G., Feinstein, C. N., Freeland, S. L., Friedlaender, F. M., Hoffmann, C. H., Hurlburt, N. E., Jurcevich, B. K., Katz, N. L., Kelly, G. A., Lemen, J. R., Levay, M., Lindgren, R. W., Mathur, D. P., Meyer, S. B., Morrison, S. J., Morrison, M. D., Nightingale, R. W., Pope, T. P., Rehse, R. A., Schrijver, C. J., Shine, R. A., Shing, L., Strong, K. T., Tarbell, T. D., Title, A. M., Torgerson, D. D., Golub, L., Bookbinder, J. A., Caldwell, D., Cheimets, P. N., Davis, W. N., Deluca, E. E., McMullen, R. A., Warren, H. P., Amato, D., Fisher, R., Maldonado, H. and Parkinson, C. (1999) The transition region and coronal explorer. SoPh, 187(2), 229–260. https://doi.org/10.1023/A:1005166902804.

Harra, L. K. and Sterling, A. C. (2003) Imaging and spectroscopic investigations of a solar coronal wave: Properties of the wave front and associated erupting material. ApJ, 587, 429–438. https://doi.org/10.1086/368079.

Hou, Z., Tian, H., Wang, J.-S., Zhang, X., Song, Q., Zheng, R., Chen, H., Chen, B., Bai, X., Chen, Y., He, L., Song, K., Zhang, P., Hu, X., Dun, J., Zong, W., Song, Y., Xu, Y. and Tan, G. (2022) Three-dimensional propagation of the global extreme-ultraviolet wave associated with a solar eruption on 2021 October 28. ApJ, 928(2), 98. https://doi.org/10.3847/1538-4357/ac590d.

Kaiser, M. L., Kucera, T. A., Davila, J. M., St. Cyr, O. C., Guhathakurta, M. and Christian, E. (2008) The STEREO mission: An introduction. SSRv, 136(1-4), 5–16. https://doi.org/10.1007/s11214-007-9277-0.

Kay, H. R. M., Culhane, J. L., Harra, L. K. and Matthews, S. A. (2003) Flare characteristics: Properties of eruptive and non-eruptive events and their associations. AdSpR, 32(6), 1051–1056. https://doi.org/10.1016/S0273-1177(03)00308-9.

Kerdraon, A. and Delouis, J.-M. (1997) The Nançay radioheliograph. In Coronal Physics from Radio and Space Observations, edited by Trottet, G., vol. 483 of *LNP*, pp. 192–201. Springer, Berlin, Heidelberg (DE). https://doi.org/10.1007/BFb0106458.

Klassen, A., Aurass, H., Mann, G. and Thompson, B. J. (2000) Catalogue of the 1997 SOHO-EIT coronal transient waves and associated type II radio burst spectra. A&AS, 141, 357–369. https://doi.org/10.1051/aas:2000125.

Lemen, J. R., Title, A. M., Akin, D. J., Boerner, P. F., Chou, C., Drake, J. F., Duncan, D. W., Edwards, C. G., Friedlaender, F. M., Heyman, G. F., Hurlburt, N. E., Katz, N. L., Kushner, G. D., Levay, M., Lindgren, R. W., Mathur, D. P., McFeaters, E. L., Mitchell, S., Rehse, R. A., Schrijver, C. J., Springer, L. A., Stern, R. A., Tarbell, T. D., Wuelser, J.-P., Wolfson, C. J., Yanari, C., Bookbinder, J. A., Cheimets, P. N., Caldwell, D., Deluca, E. E., Gates, R., Golub, L., Park, S., Podgorski, W. A., Bush, R. I., Scherrer, P. H., Gummin, M. A., Smith, P., Auker, G., Jerram, P., Pool, P., Soufli, R., Windt, D. L., Beardsley, S., Clapp, M., Lang, J. and Waltham, N. (2012) The Atmospheric Imaging Assembly (AIA) on the Solar Dynamics Observatory (SDO). SoPh, 275, 17–40. https://doi.org/10.1007/s11207-011-9776-8.

Li, T., Zhang, J., Yang, S. and Liu, W. (2012) *SDO*/AIA observations of secondary waves generated by interaction of the 2011 June 7 global EUV wave with solar coronal structures. ApJ, 746(1), 13. https://doi.org/10.1088/0004-637X/746/1/13.

Liu, R., Wang, Y., Lee, J. and Shen, C. (2018) Impacts of EUV wavefronts on coronal structures in homologous coronal mass ejections. ApJ, 870(1), 15. https://doi.org/10.3847/1538-4357/aaf04e.

Long, D. M., Bloomfield, D. S., Chen, P. F., Downs, C., Gallagher, P. T., Kwon, R.-Y., Vanninathan, K., Veronig, A. M., Vourlidas, A., Vršnak, B., Warmuth, A. and Žic, T. (2017a) Understanding the physical nature of coronal "EIT waves". SoPh, 292, 7. https://doi.org/10.1007/s11207-016-1030-y.

Long, D. M., DeLuca, E. E. and Gallagher, P. T. (2011) The wave properties of coronal bright fronts observed using *SDO*/AIA. ApJ, 741(1), L21. https://doi.org/10.1088/2041-8205/741/1/L21.

Long, D. M., Gallagher, P. T., McAteer, R. T. J. and Bloomfield, D. S. (2008) The kinematics of a globally propagating disturbance in the solar corona. ApJ, 680, L81–L84. https://doi.org/10.1086/589742.

Long, D. M., Murphy, P., Graham, G., Carley, E. P. and Pérez-Suárez, D. (2017b) A statistical analysis of the solar phenomena associated with global EUV waves. SoPh, 292(12), 185. https://doi.org/10.1007/s11207-017-1206-0.

Luna, M., Su, Y., Schmieder, B., Chandra, R. and Kucera, T. A. (2017) Large-amplitude longitudinal oscillations triggered by the merging of two solar filaments: Observations and magnetic field analysis. ApJ, 850(2), 143. https://doi.org/10.3847/1538-4357/aa9713.

Mackay, D. H., Karpen, J. T., Ballester, J. L., Schmieder, B. and Aulanier, G. (2010) Physics of solar prominences: II–Magnetic structure and dynamics. SSRv, 151(4), 333–399. https://doi.org/10.1007/s11214-010-9628-0.

Mann, G., Aurass, H., Klassen, A., Estel, C. and Thompson, B. J. (1999) Coronal transient waves and coronal shock waves. In 8th SOHO Workshop: Plasma Dynamics and Diagnostics in the Solar Transition Region and Corona, edited by Vial, J. C. and Kaldeich-Schü, B., vol. 446 of *ESASP*, pp. 477–481. https://ui.adsabs.harvard.edu/abs/1999ESASP.446..477M.

Miteva, R., Klein, K. L., Kienreich, I., Temmer, M., Veronig, A. and Malandraki, O. E. (2014) Solar energetic particles and associated EIT disturbances in Solar Cycle 23. SoPh, 289(7), 2601–2631. https://doi.org/10.1007/s11207-014-0499-5.

Moreton, G. E. and Ramsey, H. E. (1960) Recent observations of dynamical phenomena associated with solar flares. PASP, 72, 357–358. https://doi.org/10.1086/127549.

Muhr, N., Veronig, A. M., Kienreich, I. W., Vršnak, B., Temmer, M. and Bein, B. M. (2014) Statistical analysis of large-scale EUV waves observed by STEREO/EUVI. SoPh, 289, 4563–4588. https://doi.org/10.1007/s11207-014-0594-7.

Nakajima, H., Nishio, M., Enome, S., Shibasaki, K., Takano, T., Hanaoka, Y., Torii, C., Sekiguchi, H., Bushimata, T., Kawashima, S., Shinohara, N., Irimajiri, Y., Koshiishi, H., Kosugi, T., Shiomi, Y., Sawa, M. and Kai, K. (1994) The Nobeyama radioheliograph. IEEEP, 82(5), 705–713.

Nakariakov, V. M. and Ofman, L. (2001) Determination of the coronal magnetic field by coronal loop oscillations. A&A, 372, L53–L56. https://doi.org/10.1051/0004-6361:20010607.

Nakariakov, V. M. and Verwichte, E. (2005) Coronal waves and oscillations. LRSP, 2(1), 3. https://doi.org/10.12942/lrsp-2005-3.

Newkirk, G., Jr. (1961) The solar corona in active regions and the thermal origin of the slowly varying component of solar radio radiation. ApJ, 133, 983. https://doi.org/10.1086/147104.

Nitta, N. V., Liu, W., Gopalswamy, N. and Yashiro, S. (2014) The relation between large-scale coronal propagating fronts and type II radio bursts. SoPh, 289(12), 4589–4606. https://doi.org/10.1007/s11207-014-0602-y.

Nitta, N. V., Schrijver, C. J., Title, A. M. and Liu, W. (2013) Large-scale coronal propagating fronts in solar eruptions as observed by the Atmospheric Imaging Assembly on board the Solar Dynamics Observatory–an ensemble study. ApJ, 776, 58. https://doi.org/10.1088/0004-637X/776/1/58.

Ofman, L. and Thompson, B. J. (2002) Interaction of EIT waves with coronal active regions. ApJ, 574(1), 440–452. https://doi.org/10.1086/340924.

Olmedo, O., Vourlidas, A., Zhang, J. and Cheng, X. (2012) Secondary waves and/or the "reflection" from and "transmission" through a coronal hole of an extreme ultraviolet wave associated with the 2011 February 15 X2.2 flare observed with *SDO*/AIA and *STEREO*/EUVI. ApJ, 756(2), 143. https://doi.org/10.1088/0004-637X/756/2/143.

Pesnell, W. D., Thompson, B. J. and Chamberlin, P. C. (2012) The Solar Dynamics Observatory (SDO). SoPh, 275, 3–15. https://doi.org/10.1007/s11207-011-9841-3.

Piantschitsch, I., Vršnak, B., Hanslmeier, A., Lemmerer, B., Veronig, A., Hernandez-Perez, A., Čalogović, J. and Žic, T. (2017) A numerical simulation of coronal waves interacting with coronal holes. I. Basic features. ApJ, 850, 88. https://doi.org/10.3847/1538-4357/aa8cc9.

Piantschitsch, I., Vršnak, B., Hanslmeier, A., Lemmerer, B., Veronig, A., Hernandez-Perez, A. and Čalogović, J. (2018a) Numerical simulation of coronal waves interacting with coronal holes. II. Dependence on Alfvén speed inside the coronal hole. ApJ, 857(2), 130. https://doi.org/10.3847/1538-4357/aab709.

Piantschitsch, I., Vršnak, B., Hanslmeier, A., Lemmerer, B., Veronig, A., Hernandez-Perez, A. and Čalogović, J. (2018b) Numerical simulation of coronal waves interacting with coronal holes. III. Dependence on initial amplitude of the incoming wave. ApJ, 860(1), 24. https://doi.org/10.3847/1538-4357/aabe7f.

Pick, M., Malherbe, J.-M., Kerdraon, A. and Maia, D. J. F. (2005) On the disk Hα and radio observations of the 2003 October 28 flare and coronal mass ejection event. ApJ, 631(1), L97–L100. https://doi.org/10.1086/497137.

Podladchikova, T., Veronig, A. M., Dissauer, K., Temmer, M. and Podladchikova, O. (2019) Three-dimensional reconstructions of extreme-ultraviolet wave front heights and their influence on wave kinematics. ApJ, 877(2), 68. https://doi.org/10.3847/1538-4357/ab1b3a.

Roberts, B., Edwin, P. M. and Benz, A. O. (1984) On coronal oscillations. ApJ, 279, 857–865. https://doi.org/10.1086/161956.

Shen, Y. and Liu, Y. (2012) Evidence for the wave nature of an extreme ultraviolet wave observed by the Atmospheric Imaging Assembly on board the Solar Dynamics Observatory. ApJ, 754(1), 7. https://doi.org/10.1088/0004-637X/754/1/7.

Shen, Y., Liu, Y., Su, J., Li, H., Zhao, R., Tian, Z., Ichimoto, K. and Shibata, K. (2013) Diffraction, refraction, and reflection of an extreme-ultraviolet wave observed during its interactions with remote active regions. ApJ, 773(2), L33. https://doi.org/10.1088/2041-8205/773/2/L33.

Thompson, B. J., Gurman, J. B., Neupert, W. M., Newmark, J. S., Delaboudinière, J. P., Cyr, O. C. S., Stezelberger, S., Dere, K. P., Howard, R. A. and Michels, D. J. (1999) SOHO/EIT observations of the 1997 April 7 coronal transient: Possible evidence of coronal Moreton waves. ApJ, 517(2), L151–L154. https://doi.org/10.1086/312030.

Thompson, B. J. and Myers, D. C. (2009) A catalog of coronal "EIT wave" transients. ApJ, 183, 225–243. https://doi.org/10.1088/0067-0049/183/2/225.

Thompson, B. J., Plunkett, S. P., Gurman, J. B., Newmark, J. S., St. Cyr, O. C. and Michels, D. J. (1998) SOHO/EIT observations of an Earth-directed coronal mass ejection on May 12, 1997. GeoRL, 25, 2465–2468. https://doi.org/10.1029/98GL50429.

Thompson, B. J., Reynolds, B., Aurass, H., Gopalswamy, N., Gurman, J. B., Hudson, H. S., Martin, S. F. and St. Cyr, O. C. (2000) Observations of the 24 September 1997 coronal flare waves. SoPh, 193, 161–180. https://doi.org/10.1023/A:1005222123970.

Torsti, J., Kocharov, L. G., Teittinen, M. and Thompson, B. J. (1999) Injection of $\gtrsim 10$ MeV protons in association with a coronal Moreton wave. ApJ, 510(1), 460–465. https://doi.org/10.1086/306581.

Tripathi, D. and Raouafi, N. E. (2007) On the relationship between coronal waves associated with a CME on 5 March 2000. A&A, 473(3), 951–957. https://doi.org/10.1051/0004-6361:20077255.

Uchida, Y. (1968) Propagation of hydromagnetic disturbances in the solar corona and Moreton's wave phenomenon. SoPh, 4(1), 30–44. https://doi.org/10.1007/BF00146996.

Uchida, Y. (1970) Diagnosis of coronal magnetic structure by flare-associated hydromagnetic disturbances. PASJ, 22, 341–346.

van Driel-Gesztelyi, L., Goff, C. P., Démoulin, P., Culhane, J. L., Matthews, S. A., Harra, L. K., Mandrini, C. H., Klein, K. L. and Kurokawa, H. (2008) Multi-scale reconnections in a complex CME. AdSpR, 42(5), 858–865. https://doi.org/10.1016/j.asr.2007.04.065.

Veronig, A. M., Muhr, N., Kienreich, I. W., Temmer, M. and Vršnak, B. (2010) First observations of a dome-shaped large-scale coronal extreme-ultraviolet wave. ApJ, 716(1), L57–L62. https://doi.org/10.1088/2041-8205/716/1/L57.

Veronig, A. M., Temmer, M. and Vršnak, B. (2008) High-cadence observations of a global coronal wave by *STEREO* EUVI. ApJ, 681, L113–L116. https://doi.org/10.1086/590493.

Vršnak, B., Magdalenić, J., Temmer, M., Veronig, A., Warmuth, A., Mann, G., Aurass, H. and Otruba, W. (2005) Broadband metric-range radio emission associated with a Moreton/EIT wave. ApJ, 625(1), L67–L70. https://doi.org/10.1086/430763.

Wang, J., Yan, X., Xue, Z., Yang, L., Li, Q., Xu, Z., Yang, L. and Peng, Y. (2022) Two homologous quasi-periodic fast-mode propagating wave trains induced by two small-scale filament eruptions. ApJ, 936(1), L12. https://doi.org/10.3847/2041-8213/ac8b79.

Wang, Y.-M. (2000) EIT waves and fast-mode propagation in the solar corona. ApJ, 543, L89–L93. https://doi.org/10.1086/318178.

Warmuth, A. (2015) Large-scale globally propagating coronal waves. LRSP, 12, 3. https://doi.org/10.1007/lrsp-2015-3.

Warmuth, A. and Mann, G. (2011) Kinematical evidence for physically different classes of large-scale coronal EUV waves. A&A, 532, A151. https://doi.org/10.1051/0004-6361/201116685.

Warmuth, A., Mann, G. and Aurass, H. (2005) First soft X-ray observations of global coronal waves with the GOES Solar X-ray Imager. ApJ, 626(2), L121–L124. https://doi.org/10.1086/431756.

Warmuth, A., Vršnak, B., Magdalenić, J., Hanslmeier, A. and Otruba, W. (2004) A multi-wavelength study of solar flare waves. I. Observations and basic properties. A&A, 418, 1101–1115. https://doi.org/10.1051/0004-6361:20034332.

Warmuth, A., Vršnak, B., Aurass, H. and Hanslmeier, A. (2001) Evolution of two EIT/Hα Moreton waves. ApJ, 560(1), L105–L109. https://doi.org/10.1086/324055.

White, S. M., Balasubramaniam, K. and Cliver, E. (2013) Direct comparison of a solar Moreton wave, EUV wave and CME. Tech. Rep. AFRL-RV-PS-TP-2014-0004, Air Force Research Laboratory, Kirtland Air Force Base (NM).

Wills-Davey, M. J., DeForest, C. E. and Stenflo, J. O. (2007) Are "EIT waves" fast-mode MHD waves? ApJ, 664(1), 556–562. https://doi.org/10.1086/519013.

Wills-Davey, M. J. and Thompson, B. J. (1999) Observations of a propagating disturbance in TRACE. SoPh, 190, 467–483. https://doi.org/10.1023/A:1005201500675.

Wu, S. T., Zheng, H., Wang, S., Thompson, B. J., Plunkett, S. P., Zhao, X. P. and Dryer, M. (2001) Three-dimensional numerical simulation of MHD waves observed by the Extreme Ultraviolet Imaging Telescope. JGR, 106(A11), 25089–25102. https://doi.org/10.1029/2000JA000447.

Yang, L., Zhang, J., Liu, W., Li, T. and Shen, Y. (2013) *SDO*/AIA and *Hinode*/EIS observations of interaction between an EUV wave and active region loops. ApJ, 775(1), 39. https://doi.org/10.1088/0004-637X/775/1/39.

Zheng, R., Chen, Y., Feng, S., Wang, B. and Song, H. (2018) An extreme-ultraviolet wave generating upward secondary waves in a streamer-like solar structure. ApJ, 858(1), L1. https://doi.org/10.3847/2041-8213/aabe87.

Zheng, R., Wang, B., Zhang, L., Chen, Y. and Erdélyi, R. (2022) Twin extreme ultraviolet waves in the solar corona. ApJ, 929(1), L4. https://doi.org/10.3847/2041-8213/ac61e3.

Zhou, X., Shen, Y., Tang, Z., Zhou, C., Duan, Y. and Tan, S. (2022) Total reflection of a flare-driven quasi-periodic extreme ultraviolet wave train at a coronal hole boundary. A&A, 659, A164. https://doi.org/10.1051/0004-6361/202142536.

Zhukov, A. N. and Auchère, F. (2004) On the nature of EIT waves, EUV dimmings and their link to CMEs. A&A, 427, 705–716. https://doi.org/10.1051/0004-6361:20040351.

Zhukov, A. N., Rodriguez, L. and de Patoul, J. (2009a) STEREO/SECCHI observations on 8 December 2007: Evidence against the wave hypothesis of the EIT wave origin. SoPh, 259, 73–85. https://doi.org/10.1007/s11207-009-9375-0.

Zhukov, A. N., Rodriguez, L. and de Patoul, J. (2009b) STEREO/SECCHI observations on 8 December 2007: Evidence against the wave hypothesis of the EIT wave origin. SoPh, 259(1-2), 73–85. https://doi.org/10.1007/s11207-009-9375-0.

Zong, W. and Dai, Y. (2017) Mode conversion of a solar extreme-ultraviolet wave over a coronal cavity. ApJ, 834, L15. https://doi.org/10.3847/2041-8213/834/2/L15.